Journal of Operation and Automation in Power Engineering

Vol. 8, No. 1, Feb. 2020, Pages: 75-85

http://joape.uma.ac.ir

# SCA based Fractional-Order PID Controller Considering Delayed EV Aggregators

*F. Babaei* [*]*and A. Safari*

*Department of Electrical Engineering, Shahid Madani Azarbaijan University, Tabriz, Iran.*

***Abstract-*** *The EVs battery has the ability to enhance the balance between the load demand and power generation units. The EV aggregators to manage the random behaviour of EV owners and increasing EVs participation in the ancillary services market are employed. The presence of aggregators could lead to time-varying delay in load frequency control (LFC) schemes. The effects of these delays must be considered in the LFC controller design. Due to the dependency of controller effectiveness on its parameters, these parameters should be designed in such a way that the LFC system has desired performance in the presence of time-varying delay. Therefore, a Sine Cosine Algorithm (SCA) is utilized to adjust the fractional-order PID (FOPID) controller coefficients. Also, some evaluations are performed about the proposed LFC performance by integral absolute error (IAE) indicator. Simulations are carried out in both single and two area LFC system containing EV aggregators with time-varying delay. According to results, the proposed controller has fewer frequency variations in contrast to other controllers presented in the case studies. The obtained output could be considered as a solution to evaluate the proposed controller performance for damping the frequency oscillations in the delayed LFC system.*

***Keyword:*** Electric vehicle aggregator, Fractional-order PID, Load frequency control, Sine cosine algorithm, Time-varying delay.

## NOMENCLATURE

| | |
|---|---|
| EV | Electric Vehicle |
| FOPID | Fractional-Order PID Controller |
| IAE | Integral Absolute Error |
| LFC | Load Frequency Control |
| SCA | Sine Cosine Algorithm |
| $\alpha_0$ | Participation Ratio of Generator |
| $\alpha_i$ | Participation Ratio of $i^{th}$ aggregator |
| $K_{ev}$ | EV Battery Gain |
| $T_{ev}$ | EV Battery Time Constant |
| $\tau(t)$ | Time varying Delay |
| R | Speed Regulation Factor |
| M | Inertia Constant |
| D | Load-Damping Factor |
| $T_g$ | Governor Time Constant |
| $T_c$ | Turbine Time Constant |
| $x(t)$ | System State Vector |
| $T_r$ | Reheat Time Constant |
| $F_r$ | Fraction of Total Turbine Power |
| $\beta$ | Frequency Bias Factor |
| $\Delta f$ | Frequency Variation |
| $\Delta X_g$ | Valve Position Variation |
| $\Delta P_m$ | Mechanical Power Output Variation |
| $\Delta P_g$ | Generator Power Output Variation |
| $\Delta P_{ev,k}$ | Power Output Variation of k-th Aggregator |
| $\Delta P_d$ | Load Disturbance |
| $\lambda$ | FOPID Integral Term Order |
| $\mu$ | FOPID Derivative Term Order |
| $X_i^t$ | Position of the Current Solution |
| $P_i^t$ | Position of the Destination Point |
| *diag* | Block-Diagonal Matrix |

Received: 21 May. 2019
Revised: 04 July. 2019
Accepted: 15 July. 2019
*Corresponding author:
E-mail: f.babaei@azaruniv.ac.ir (F. Babaei)
Digital object identifier: 10.22098/joape.2019.5244.1390
***Research Paper***


## 1. INTRODUCTION

According to the Paris Agreement in December 2015, each country could freely decrease its greenhouse gas emissions along a pathway that works to achieve this goal [1]. One of the main reasons of air pollution is fossil fuel power plants. Replacing these units with renewable energy resources and Electric Vehicles (EVs) could significantly lead to reducing greenhouse gas emissions. On the other hand, fuel cost increment, oil insufficiency and battery technology improvement have enhanced the investment cost in the EVs sector. Thus, it is estimated that fossil fuelled vehicles will be replaced with EVs faster in coming years. The widespread use of the EVs could result in imposing unknown and unexpected load patterns on the power system load profile. So, the power system infrastructure must be designed in such a way that makes a response to the high power of EVs charging processes. Different aspects of EVs should be analyzed in order to exploit their advantages in power systems. For example, in Ref. [2], some information is collected from Switzerland utility companies and some researches are performed about the effects of EV charging on the high-voltage grid. The widespread penetration of EVs could significantly affect the system peak load and power plant dispatch. Moreover, the life expectancy of power system elements relies on the EVs amount and charging [3]. Due to Ref. [4], utilizing the Vehicle-to-Grid (V2G) technique causes some delays for investing in the construction of conventional power plants. Developing the smart grid concept makes the EVs main role, especially in the form of the V2G technique, more obvious. By using the V2G technology, EVs are able to return the stored power in their idle time (park time) to the network at a load peak time [5]. As mentioned in Ref. [6], active and reactive power compensation, frequency control, peak load correction are the examples of services which are prepared for the power system by V2G technique. The communication networks that transfer the control signal to EVs could lead to time-varying delays. It should be noted that the delay-dependent stability of the load frequency control (LFC) system in the presence of the EV aggregators must be regarded more. Because of the enormous participation of EVs and their management, there is a need for an accountable agent which is called EVs aggregator. Actually, an EVs aggregator acts as an intermediary between the independent system operator and EVs owners which is frequently trying to maximize its interests and EVs owners by participating in ancillary services markets [7]. In terms of controlling methods, LFC schemes are sorted into different types which are discussed in continuing. An optimal distributed multi-agent LFC controller is designed by Ref. [8]. This controller parameters are optimized using Grey Wolf Optimization algorithm. An analytical PID controller based on the fractional-order internal model control method is introduced to improve the power system performance [9]. The coordinated control between the EVs based LFC system and the traditional LFC system in the frequency control service of a power system is proposed in Ref. [10]. Owing to this approach, when the system parameters variations get out of the determined range, the LFC system contains EVs could facilitate reaching outcome fast to frequency stability. The design of the new EVs based on the LFC scheme for a multi-area system which includes various transmission links, intelligent infrastructure and discharged EVs technology is presented in Ref. [11]. First, the dynamic model of mentioned power system is gained. Next, the charge or discharge rate of EVs and also the output power of the unit are optimally achieved by using state feedback control method. A decentralized control structure is proposed for EVs to improve the primary and supplementary frequency control of the power system [12]. Due to the state-of-art methods of controllable loads modelling, a new lumped model of EVs is presented in the Ref. [13]. This model considers all the available data of EVs to attain a desirable state of charge (SOC) for the EV station. Then, the effectiveness of the proposed model is examined in a hybrid power system. A different combination of the fuzzy logic and other classic controllers like PI, PD and cascade PI-PD construct the complementary controllers which could be used as a secondary LFC in microgrids. In Ref. [14], the FPD/PI-PD controller restrains the frequency oscillation of area satisfactorily. Moreover, IJAYA algorithm is decided to be used for designing the suggested controller. Due to Ref. [15], currently, the coefficient diagram method which is known as one of the robust virtual inertia controls is implemented in the microgrid with high influence on renewable energy resources. Recently, EV batteries are introduced as a solution for controlling the microgrids frequency. In accordance with renewable energy resources progressing and their random nature, V2G has to perform correctly in a bigger range in contrast to the previous operating situation. To reach this purpose, Ref. [16] proposes a novel multi-objective fractional-order controller. PID controller adjusted by the particle swarm optimization (PSO) stands on the artificial neural network technique is a great choice which is utilized as the LFC controller in an island microgrid [17]. In the LFC system, communication networks send the control instructions to EVs. Time-varying delays between different parts of system for example dispatching center, EVs aggregator, power station and etc. may be the result of the smart grid development and communication infrastructures employment. In Ref. [18], numerous time-varying delays and system uncertainties are observed in system modelling. Moreover, to ensure the frequency control, a robust static output feedback based on LFC controller is presented. Some analyses are performed about the effects of the communication delays on frequency control of the multi-area power systems consisted from plug-in EV in Ref. [19]. First, the plug-in EV owners' behaviour, battery and delay characteristics are all important factors which conclude a dynamic model of the plug-in EVs. Next, the time delays and system uncertainties are added to a state-space model of the power system and finally, a robust PID based on LFC controller is proposed. It should be noted that the mentioned controller is designed by using a linear matrix inequality and PSO algorithm. The EVs remarkable participation in ancillary service, especially frequency control, brings about the power market restructuring. In other word, the power imbalance in the different areas could be compensated with the help of EVs batteries denominated as a modern type of energy storage systems in the situation in which the power market agreements are violated. Ref. [20] reports about the EVs participation in the LFC system besides other traditional power generation units under a deregulated condition. The application of the fractional order controller optimized by the flower pollination algorithm has been proposed in Ref. [21]. Although the performance of the controller is presented, the simple model for EV and ignoring other controllable loads reduce the value of that study. The robust LFC scheme is accomplished for mentioned system using by the EVs aggregated model and improved fractional order controller. In Ref. [22], the FOPI controller for single-area LFC system with time delay is presented. Some studies are performed on a robust LFC system for single-area power system with evaluating the uncertainties and time delays in data transfer in Ref. [23]. Delay-dependent stability analysis of LFC system containing EV aggregators with single and multiple time-varying delays are studied in Ref. [24]. In order to reduce the negative effects of time-varying delay in LFC system performance, the controller gain must be optimally specified with regard the existed data on numerous time-varying delays. In this paper, optimal fractional order PID (FOPID) controller is used as a LFC system to reach the controlling purposes. In order to design the presented controller coefficients and participation ratio of each EVs aggregator, Sine Cosine algorithm (SCA) is utilized. In this case, the LFC system structure is somehow that minimizes the integral absolute error (IAE) indicator. It should be mentioned that the IAE is usually employed not only to reduce the system error, but also to find the best controller parameters.

The contributions of this paper can be stated as follows:

- Using of EVs aggregator to assist the current power systems in eliminating the load variations.
- An optimal controller design for the LFC scheme in attendance of the delayed EV aggregator.
- Investigating the effect of time-varying delays in the modified LFC model.
- Optimal allocation of the participation ratio of the generator and EVs aggregator by considering the interaction between the delay margin, controller gain

The framework of this paper is organized as follows. The dynamic model of the LFC system including EV aggregators is presented in Section 2. Section 3 discusses about the SCA algorithm to be used in the FOPID controller design in single and two area LFC model consisting time-varying delay. Section 4 focuses on simulating the results of different scenarios. Finally, Section 5 is allocated to conclusions..

## 2. PROBLEM STATEMENT

It is supposed that the EV aggregators have the ability to provide the frequency control service by many available EVs. From the viewpoint of the system operator, the EVs aggregator is a great generation or demand unit which may improve the performance of LFC system. Thus, the random behaviour of a single EV owner is not observed in the LFC system. Figure 1 displays the EVs aggregator position in the power system performance.

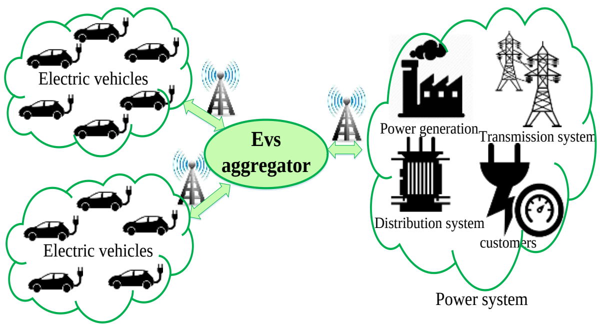


**Fig. 1. The EVs aggregator as a middleman term between the power system and EVs**

In accordance with Fig. 1, the control center sends the commands to the EVs aggregator to eliminate the frequency oscillations. After receiving the control commands, EVs aggregator determines the contribution of each available EVs to take a part in frequency control service. Data transfer is accomplished in the system through the open communication network containing different time delay characteristics. Therefore, each EV has a delayed response. Different types of traditional LFC schemes have been presented in previous literature. A scheme of single-area LFC consisting many EVs aggregators with time-variable delays is indicated in Fig. 2. According to Fig. 2, $\alpha_0$ , $\alpha_1, \alpha_2, \ldots and\, \alpha_N$ are contribution factors of generator and each EV aggregators in the frequency control service, respectively. The synchronous generator is a converter that transforms the input mechanical power into electrical power. In this paper, reheat thermal turbine which has been equipped with the governor system is responsible to generate the mechanical input power. The thermal power generation unit including the synchronous generator, reheat thermal turbine and governor is indicated in Fig. 2.

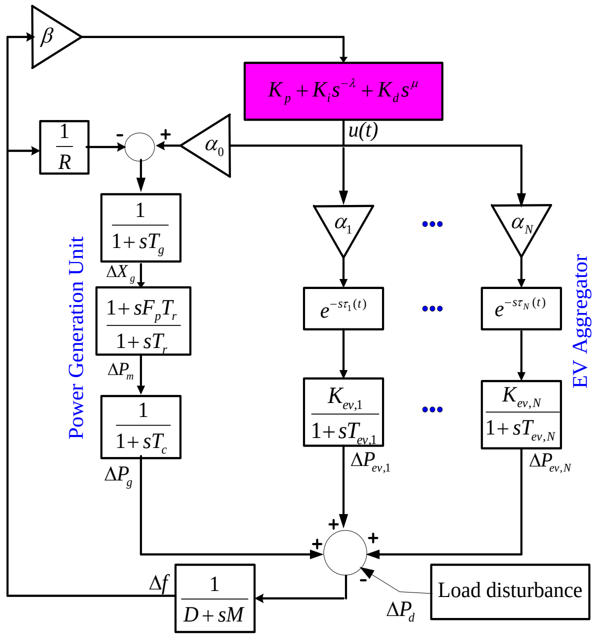


**Fig. 2. General model of modified LFC system**

### 2.1. Formulation of EV aggregators with time-varying delay

The EV owner participation in frequency control service under EVs aggregators improves the system performance. The dynamic model of EV could be formulated as [24]:

$$H_{ev}(s) = \frac{K_{ev}}{1+sT_{ev}} \tag{1}$$

Where, $K_{ev}$ and $T_{ev}$ are referred to the gain of EV battery and time constant, respectively. In this paper, EVs with high or low state of charge are ignored in the aggregator account. Thus, EVs aggregator is modeled by a first-order transfer function. In mentioned LFC system, delay is defined as the time duration of receiving control commands from EVs aggregator. It means, using infrastructure in an open communication network causes time-varying delay in the data transferring process. $e^{-s\tau(t)}$ is employed for modeling the occurred delay in sending the control signal from EVs aggregator. The time-varying delay is specified by $\tau(t)$ in this transfer function. This paper proposes the sine wave function with determined parameters for modeling the time-varying delay. The equations of the single-area LFC scheme with $N$ numbers of EVs aggregators are revealed as:

$$\dot{x}(t) = \begin{bmatrix} \Delta\dot{f} \\ \Delta\dot{X}_g \\ \Delta\dot{P}_m \\ \Delta\dot{P}_g \\ \Delta\dot{P}_{ev,1} \\ \vdots \\ \Delta\dot{P}_{ev,N} \end{bmatrix} = \begin{bmatrix} \frac{-D}{M} & 0 & 0 & \frac{1}{M} & \frac{1}{M} & \cdots & \frac{1}{M} \\ \frac{-1}{RT_g} & \frac{-1}{T_g} & 0 & 0 & 0 & \cdots & 0 \\ \frac{-F_p}{RT_g} & \frac{T_g - F_pT_r}{T_rT_g} & \frac{-1}{T_r} & 0 & 0 & \cdots & 0 \\ 0 & 0 & \frac{1}{T_c} & \frac{-1}{T_c} & 0 & \cdots & 0 \\ 0 & 0 & 0 & 0 & \frac{-1}{T_{ev,1}} & \cdots & 0 \\ \vdots & \vdots & \vdots & \vdots & \ddots & \cdots & \vdots \\ 0 & 0 & 0 & 0 & 0 & \cdots & \frac{-1}{T_{ev,N}} \end{bmatrix} \begin{bmatrix} \Delta f \\ \Delta X_g \\ \Delta P_m \\ \Delta P_g \\ \Delta P_{ev,1} \\ \vdots \\ \Delta P_{ev,N} \end{bmatrix}$$

$$+ \begin{bmatrix} 0 \\ \frac{\alpha_0}{T_g} \\ \frac{F_p\alpha_0}{T_g} \\ 0 \\ 0 \\ \vdots \\ 0 \end{bmatrix} u(t) + \sum_{j=1}^{N} \frac{\alpha_j K_{ev,j}}{T_{ev,j}} . u(t - \tau_k(t)) + \begin{bmatrix} \frac{-1}{M} \\ 0 \\ 0 \\ 0 \\ 0 \\ \vdots \\ 0 \end{bmatrix} \Delta P_d$$

$$y = \begin{bmatrix} \beta & 0 & 0 & 0 & 0 & \ldots & 0 \end{bmatrix} x(t) \tag{2}$$

### 2.2. FOPID controller

Unlike the conventional PID, the FOPID is a non-integer order controller with two extra freedom degrees. These advantages enhance the discretion of the control systems design. Flexibility and durability of the controller may be the main reasons of using FOPID in the LFC system. Eq. (3) represents the FOPID controller transfer function.

$$H_c(s) = K_p + K_i s^{-\lambda} + K_d s^{\mu} \tag{3}$$

Where, $\lambda$ and $\mu$ detect the integral and derivative term orders, respectively. Refer to Fig. 3, it could be realized that the conventional PID controller is a specific state of FOPID controller. FOPID controller performs as a PID controller whenever $\lambda$ and $\mu$ are equal to one. The main objective function which is employed to design the FOPID controller parameters and EVs aggregator participation ratio optimally is defined by Eq. (4).

It should be mentioned that the frequency oscillation increases the integral expression for either positive or negative errors. Thus, the objective function is employed with the purpose of investigating the efficiency of the FOPID controller to remove the frequency oscillation in the presence of time-varying delay.

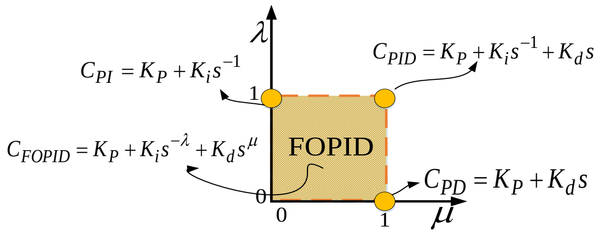


**Fig. 3. The operational area of FOPID controller**

$$OF = IAE = \int_0^{\infty} |e(t)|\, dt \tag{4}$$

## 3. SINE COSINE ALGORITHM

The optimization process in the population-based methods is starting up with a set of accidental solutions. This initial random set is repeatedly checked out by an objective function. Then, a random solution is slowly improved. Finally, the optimal solution is obtained with a set of rules which are known as the core of optimization techniques. According to the stochastic search of the population-based optimization techniques for calculating the optimization solution, achieve the optimal solution in a single run does not seem logical. In other words, there is no guarantee of outcoming a solution in the first run. In order to increase the probability of obtaining the global optimum, this process must be iterated with enough number of random solutions and generation. As mentioned, in all stochastic population-based optimization methods, the optimization process is divided into two stages: exploration versus exploitation.

At first, many random solutions to reach the hopeful regions of the search space are checked out. Unlike the former step, the random variations of the exploitation stage have been significantly reduced. In this paper, the current position of each solution is updated by Eq. 5:

$$\begin{aligned} X_i^{t+1} &= X_i^t + r_1 \times \sin(r_2) \times \left| r_3 P_i^t - X_i^t \right| \\ X_i^{t+1} &= X_i^t + r_1 \times \cos(r_2) \times \left| r_3 P_i^t - X_i^t \right| \end{aligned} \tag{5}$$

$$X_i^{t+1} = \begin{cases} X_i^t + r_1 \times \sin(r_2) \times \left| r_3 P_i^t - X_i^t \right| & r_4 < 0.5 \\ X_i^t + r_1 \times \cos(r_2) \times \left| r_3 P_i^t - X_i^t \right| & r_4 \geq 0.5 \end{cases} \tag{6}$$

Where, $X_i^t$ demonstrates the position of the current solution in $i^{th}$ dimension and $t^{th}$ iteration. Also, $P_i^t$ indicates the position of the destination point. It should be noted that $r_1, r_2$ and $r_3$ are fortuitous values. These equations for using in the SCA algorithm are combined by Eq. 6.

As seen, the SCA algorithm has four main parameters ( $r_1, r_2, r_3$ and $r_4$ ). The motion direction which is included the space between the solution and the goal is determined by parameter $r_1$ . The amount of movement towards or outwards the global solution depends on the parameter $r_2$ . The parameter $r_3$ shows the effect of destination in defining the distance to the goal. Also, the parameter $r_4$ changes between the sine and cosine parts equally. Because of the using the sine and cosine components in this formulation, this algorithm is known as Sine Cosine algorithm [25]. The impact of the sine and cosine components on the Eq. (5) and Eq. (6) in [−2, 2] is illustrated in the Fig. 4. According to Fig. 4, the effect of the range variations of sine and cosine functions leads to achieving a solution to update its position (outside or inside of the search space). An efficient algorithm discovers the hopeful regions of the search space by balancing exploration and exploitation. For this purpose, the range of sine and cosine is modified effectively via the following equation:

$$r_1 = a - t\frac{a}{T} \tag{7}$$

Where, $t$ and $T$ indicate the current and maximum iteration, respectively. Also, $a$ is a constant value.

The SCA theoretically could determine the global best solution in many optimization problems due to the following reasons:

- Creating a set of possible solutions for a specified problem and improving them,
- The intrinsic superiority of this algorithm compared to individual-based algorithms in the field of exploration and local optimum solution avoidance,
- Exploration of all areas of the search space when sine and cosine function places outside of [-1,1],
- Using the adaptive range of the sine and cosine leads to smoother crossing from exploration to exploitation,
- Storing the global optimum best estimation as the destination point during the optimization process,
- Updating the position of each solution around the current best solution and tends to achieve the promising regions of the search spaces,
- Considering the optimization problem as black boxes within the SCA algorithm and its capability to use in different problems,

- Finally, the using of the SCA algorithm results in the global best solution access and local solutions evasion. For better understanding, the flowchart of SCA is illustrated in Fig. 5.

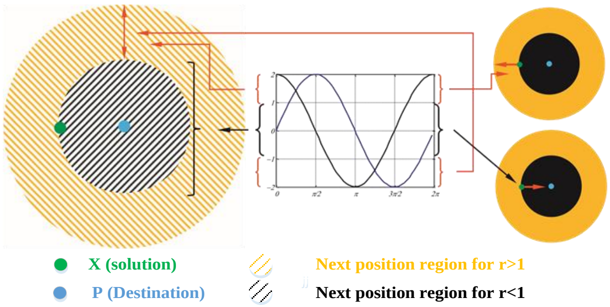


**Fig.4. Effects of Sine and Cosine component in option best solution**

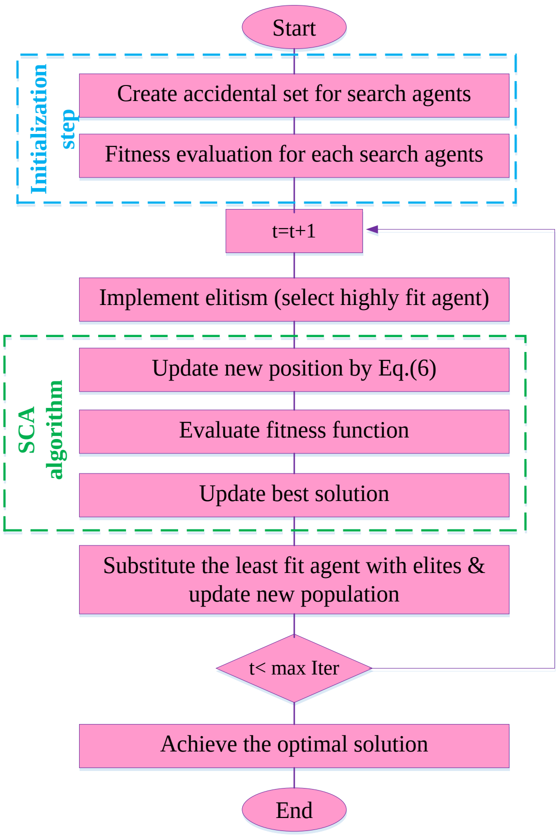


**Fig. 5. The flowchart of SCA**

## 4. SIMULATION RESULTS

In this section, several scenarios are considered. To evaluate and analyze the performance of the designed framework, the LFC system presented in Fig. 2 is simulated using MATLAB software. To illustrate the efficiency of the proposed approach, the obtained results are compared to other controllers. The proposed controller is employed in single and two-area LFC system with EV aggregators consisting time-varying delays. An equivalent generator and EV aggregator are considered instead of all generator and EV aggregators in each area, respectively. As explained in Ref. [20], the delay sensitivity of conventional generators is much less in contrast to EV aggregators. On the other hand, the contribution of fast-response resources like EV aggregators with unknown open communication network delay in the LFC system must be noted more because of their effects on the system stability. In this paper, sin wave function is utilized to model the time-varying delay. The amplitude and bias of a sine wave are both equal to 2. The employed parameters in the mentioned LFC system are designated in Appendix A.

### 4.1. One-area LFC system

The small signal stability of the LFC system could be a good benchmark for evaluating the controller effectiveness in the attendance of the EV aggregator with time-varying delay. In this paper, the integral absolute error to analyze the LFC system performance is used. It should be noted that the expressed index value should be small enough to ensure the LFC system stability. Due to the dependency of the LFC system performance on controller parameters, these parameters should be optimally designed. Moreover, decision variables like the participation ratio of the generator and EV aggregators must be determined in some way to getting better the LFC system performance. Therefore, the SCA is utilized to optimize the FOPID controller parameters and the expressed participation ratios. In order to evaluate the efficiency of the proposed controller, the PSO and SCA based PID, PSO and SCA based FOPID controller, are all simulated and presented. Finally, the obtained results are compared to each other.

***Scenario 1:*** The multi-step load variation which is exerted to LFC scheme as disturbance is displayed in Fig. 6. Figures 7-9 illustrate the frequency variation, power variation of the EV aggregator and generator by using of the PSO-PID, PSO-FOPID, SCA-PID and SCA-FOPID controllers. As it is clear, by applying the proposed controller, not only the settling time and overshoot of the error signal are both reduced but also, the oscillation occurred because of load disturbance could be wiped out significantly in the LFC scheme. Due to the large step of load disturbance signal at $t = 60\,\text{sec}$, it may be a good criterion to recognize the affectivity of controller for eliminating the frequency oscillations. FOPID controller can even improve the LFC scheme performance for removing the load disturbance. The optimal performance of these approaches depends on the IAE indicator value. In simple terms, the optimal performance of the LFC scheme is possible if the IAE indicator is close to zero.

The optimal values of the controller parameters, the generator and EVs aggregator participation ratios and also the aforementioned indicator value for each approach are listed in Table 1.

**Table 1. The obtained result for each approach**

| Parameters | PSO- PID | SCA-PID | PSO-FOPID | SCA-FOPID |
|---|---|---|---|---|
| $K_p$ | 0.5 | 0.8861 | 08109 | 0.8961 |
| $K_i$ | 0.6 | 0.43408 | 0.5 | 0.41561 |
| $K_d$ | 0.6 | 0.4188 | 0.2 | 0.36225 |
| $\lambda$ | - | - | 0.61205 | 0.9 |
| $\mu$ | - | - | 1.2599 | 0.76201 |
| $\alpha_0$ | 0.7162 | 0.76443 | 0.7557 | 0.76895 |
| $\alpha_1$ | 0.28429 | 0.24314 | 0.32939 | 0.24657 |
| IAE | 0.00696 | 0.0095 | 0.0154 | 0.0066 |

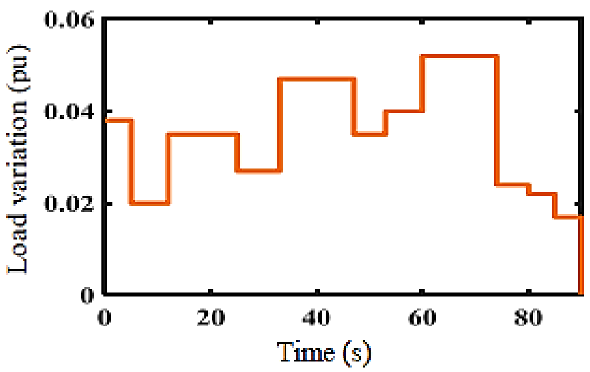


**Fig. 6. Load variations**

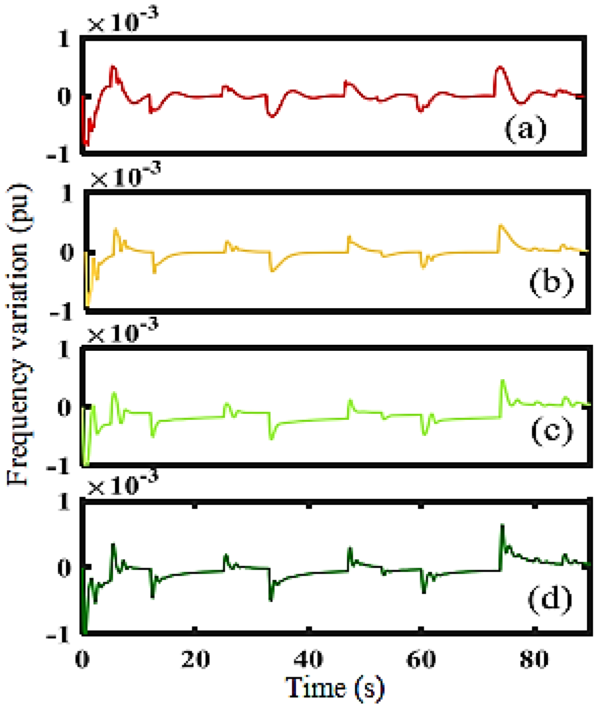


**Fig. 7. Frequency variation of the LFC scheme**
**(a) PSO-PID (b) SCA-PID (c) PSO-FOPID (d) SCA-FOPID**

**Table 2. Parameter setting of the SCA-FOPID**

| Parameter | value |
|---|---|
| $a$ | 2 |
| Number of search agents | 20 |
| Maximum number of iterations | 10 |

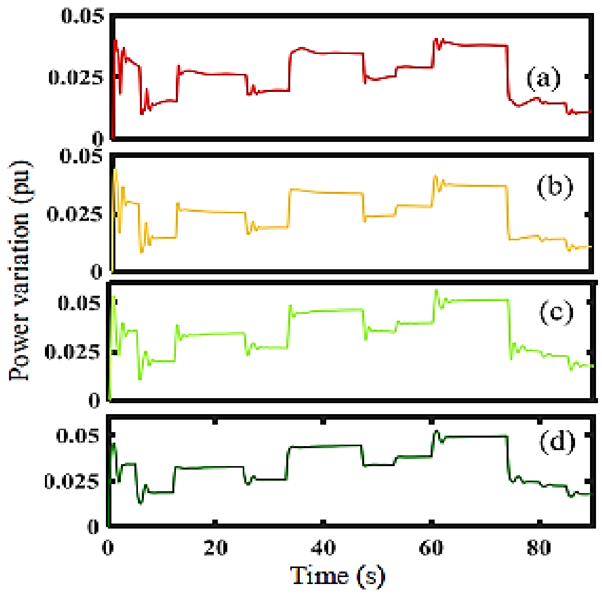


**Fig. 8. Power variation of the generator**
**(a) PSO-PID (b) SCA-PID (c) PSO-FOPID (d) SCA-FOPID**

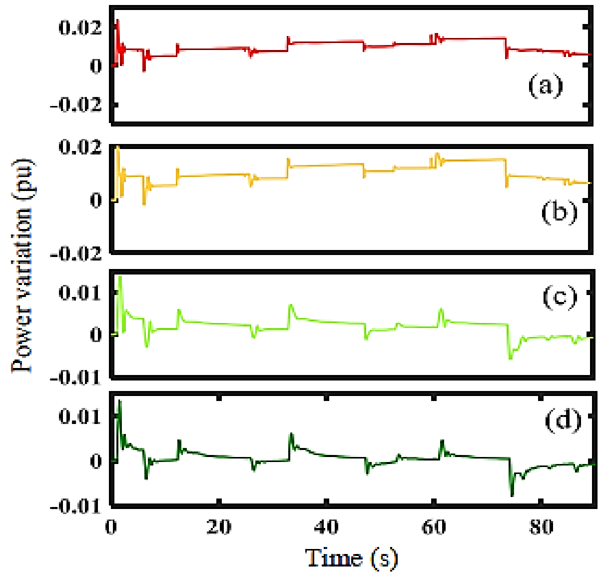


**Fig. 9. Power variation of the EV aggregator**
**(a) PSO-PID (b) SCA-PID (c) PSO-FOPID (d) SCA- FOPID**

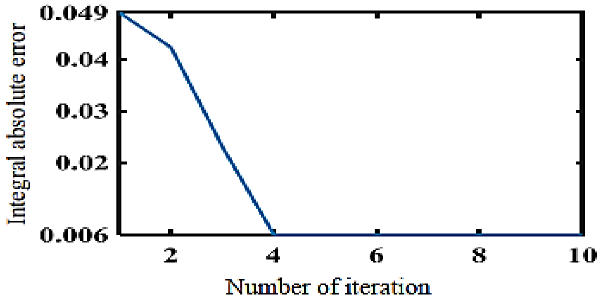


**Fig.10. Convergence curve of SCA algorithm**

**Table 3. The performance analysis of designed controllers**

| Criteria | PSO-PID | SCA-PID | PSO-FOPID | SCA-FOPID |
|---|---|---|---|---|
| IAE | 0.0064 | 0.0055 | 0.0119 | 0.0045 |

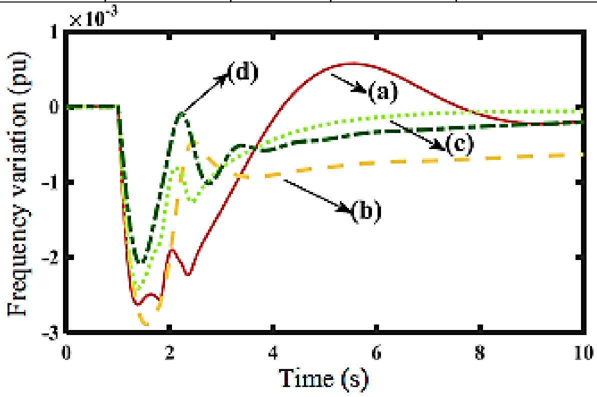


**Fig. 11. Frequency variation of the LFC scheme (a) PSO-PID (b) SCA-PID (c) PSO-FOPID (d) SCA-FOPID**

Finally, The Parameter setting of SCA-FOPID is given in Table 2. The convergent behavior derived from suggested approach is demonstrated in Fig. 10.

***Scenario 2:*** In this step, the load disturbance is considered to be constant in the LFC scheme i.e., $\Delta P_d = 0.1$ . According to Figs. 11-13, it could be concluded that the FOPID helps to reduce the peak value of frequency variation. Moreover, this decrement is obtained in the short time duration in contrast to the time duration when the PID controller is used. On the other words, the SCA-FOPID controller provides an output with a decreased amplitude in the first swing and also with the quicker damping of the frequency variation. As seen, frequency variation is well controlled via this method. The fast damping of frequency oscillation increases the lifetime of each EVs battery. Thus, it could be realized that the suggested controller has less frequency adjustment.

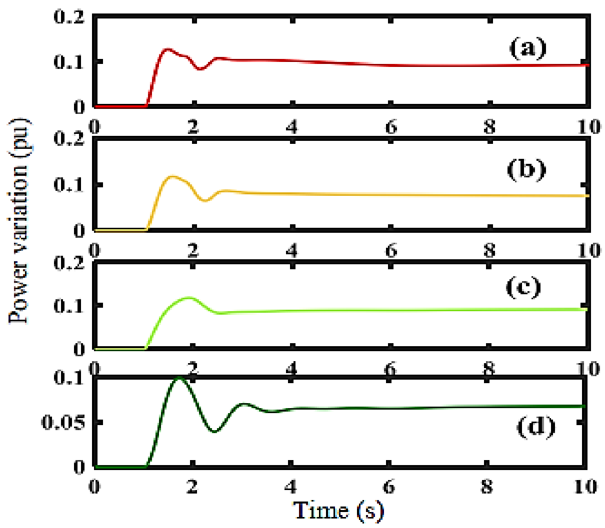


**Fig. 12. Power variation of the generator (a) PSO-PID (b) SCA-PID (c) PSO-FOPID (d) SCA-FOPID**

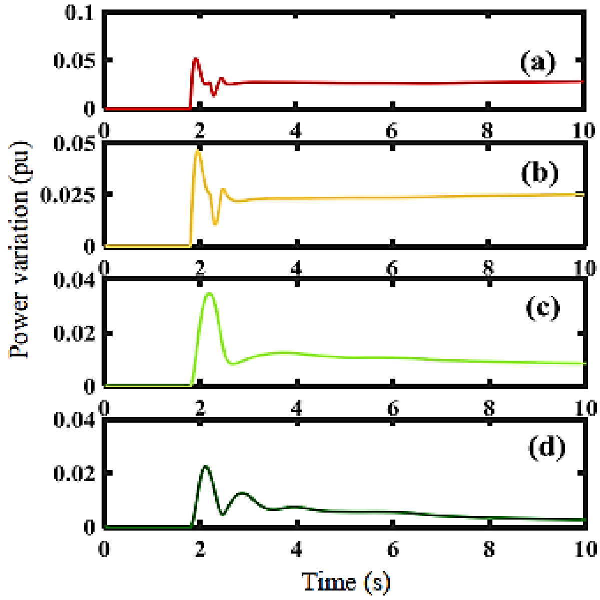


**Fig. 13. Power variation of the EV aggregator (a) PSO-PID (b) SCA-PID (c) PSO-FOPID (d) SCA-FOPID**

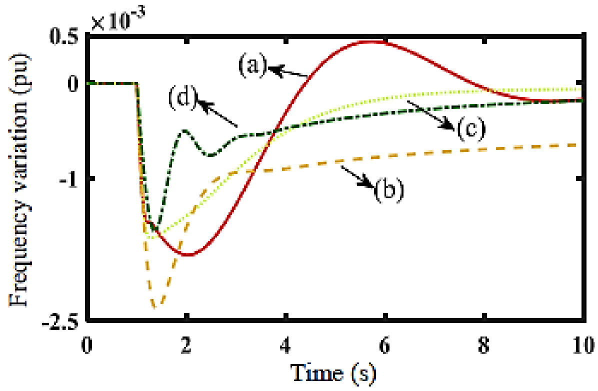


**Fig. 14. Frequency variation of the LFC scheme(a) PSO-PID (b) SCA-PID (c) PSO-FOPID (d) SCA-FOPID for $\tau(t) = e^{-2.3t}$**

In summary, this controller is employed with the purpose of reaching frequency damping with fewer overshoot and smaller settling time. Additionally, the results indicate that the IAE index value for FOPID controller has been obtained less than other methods. Table 3 demonstrates the evaluation results of these controllers.

Figure 14 shows the performance of the proposed controller for a specific function of time delays. As seen, the SCA-FOPID controller significantly eliminates the frequency oscillation for other types of time delay function ( $\tau(t) = e^{-2.3t}$ ). Also, the settling time of the error signal is remarkably decreased when the SCA-FOPID is implemented.

### 4.2. Two-area LFC system

All generators and EVs aggregators in each control area of multi-area LFC scheme are substituted by an equivalent generator and EVs aggregator, respectively.

The dynamic model of the multi-area system containing EV aggregators is given in the Appendix B. According to the two-area LFC scheme with EVs aggregator, FOPID controller is implemented to decrease the system frequency oscillation. Table 4 indicates the parameters of FOPID controller, the generator and EVs aggregator participation ratios in two-area LFC scheme which are optimally designed using by SCA.

Figure 15 shows the frequency variation of each area. Additionally, Figs. 16 and 17 illustrate the generator and EVs aggregator output power variation, respectively. The results show that the SCA-FOPID controller has well restrained the frequency oscillation caused by the load variation in the Area1 in both areas. Also, the settling time of the error signal is remarkably decreased when the SCA-FOPID is implemented.

**Table 4. Obtained results for each area using by SCA**

| Parameters | Area 1 | Area 2 |
|---|---|---|
| $K_p$ | 0.8942 | 0.8125 |
| $K_i$ | 0.3782 | 0.3697 |
| $K_d$ | 0.5 | 0.5 |
| $\lambda$ | 0.7337 | 0.69573 |
| $\mu$ | 1.4574 | 1.23 |
| $\alpha_0$ | 0.762 | 0.6155 |
| $\alpha_1$ | 0.301 | 0.39 |
| IAE | 0.00668 | 0.0002 |

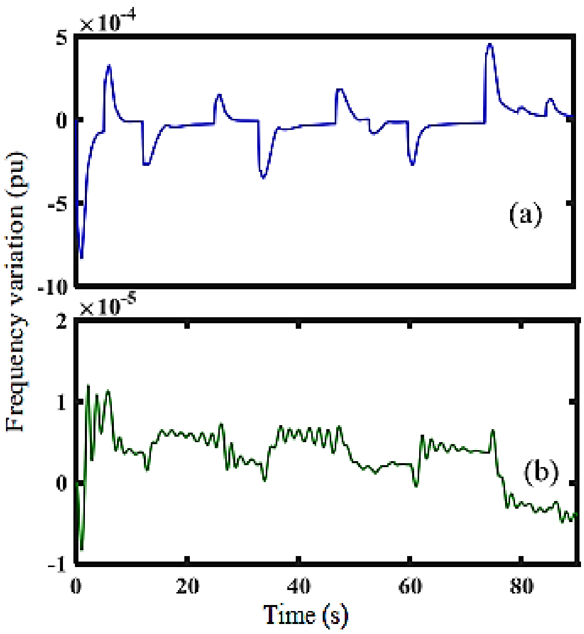


**Fig. 15. Frequency variation of the LFC scheme (a) Area 1 (b) Area 2**

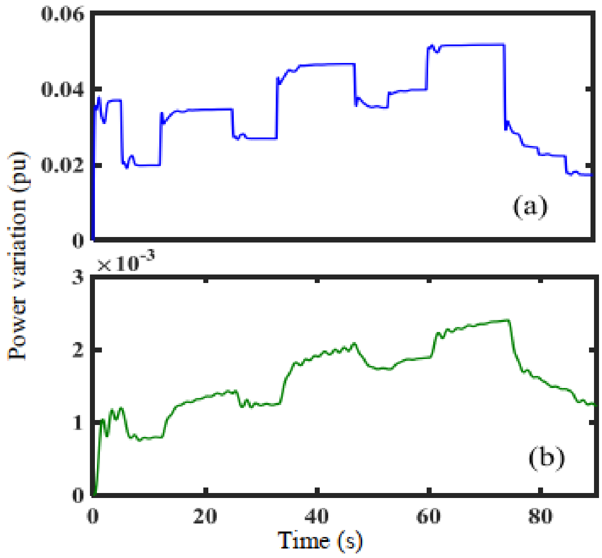


**Fig. 16. Power variation of the generator (a) Area 1 (b) Area 2**

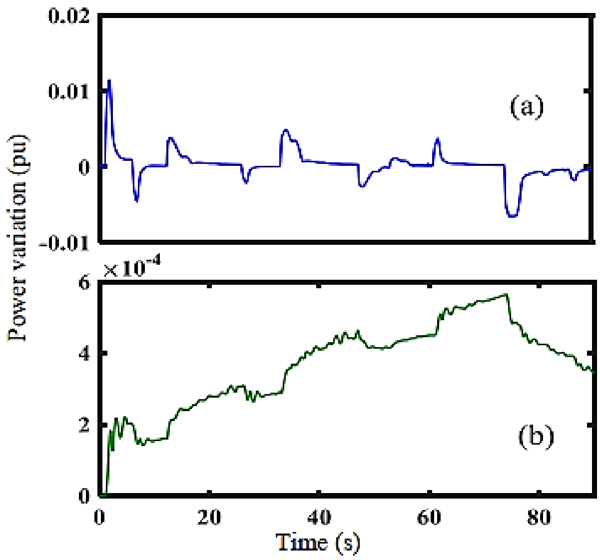


**Fig. 17. Power variation of the EV aggregator (a)Area 1 (b)Area 2**

The Area1 load disturbance which was a threat in this area, is controlled by two terms. Consequently, the effect of frequency oscillation is neutralized satisfactorily in both areas and the system performance is improved. According to the obtained results in Ref. [26], the frequency variation of the LFC system has been decreased in both step and random load change. Also, the model presented in [26] is modified by including the EVs aggregator with time varying delay.

## 5. CONCLUSIONS

The electric vehicles expansion and their more participation in ancillary services markets like frequency control service lead to enhance the efficiency of LFC models. The communication infrastructures which send the control commands from aggregator to all EVs could lead to time-varying delays. The effects of these delays must be considered in the LFC system stability analysis. In this paper, an effort was made to perform the ability of sine cosine algorithm for the optimal design of a FOPID controller parameters which is the desirable controller for the LFC systems. Also, the participation ratios of the generator and EVs aggregator were optimally designed by the SCA algorithm in the presence of time-varying delay. Both constant and variable load disturbances were considered as $\Delta P$ in the case studies. As, it is obvious from simulation results, SCA-FOPID controller reduces the undershoot and overshoot peak and settling time of the error signal. On the other words, this controller significantly eliminates the frequency oscillations occurred by the load uncertainty. By comparing the discussed controllers, it could be inferred that the good results from the SCA-FOPID controller have received.

Appendix A.

The parameters of the LFC system containing EV aggregator are given as:

Inertia constant: $M = 8.8$

Load-damping factor: $D = 1$

Governor time constant: $T_g = 0.2$

Turbine time constant: $T_c = 0.3$

Fraction of total turbine power: $F_p = 1.6$

Battery gain: $K_{ev} = 1$

Battery time constant: $T_{ev} = 0.1$

Speed regulation: $R = 1.11$

Frequency bias factor: $\beta = 40$

Reheat time constant: $T_r = 12$

Appendix B.

The dynamic model of the multi-area power system containing EV aggregators could written as follow:

$$\dot{x}(t) = Ax(t) + B_0 u(t) + \sum_{k=1}^{N} B_k . u(t - \tau_k(t)) + F.\Delta P_d \qquad \text{(B-1)}$$
$$y(t) = Cx(t)$$

Where

$$x_i(t) = \begin{bmatrix} \Delta f_i & \Delta P_{gi} & \Delta P_{mi} & \Delta X_{gi} & \Delta P_{evi} & \Delta P_{tie-i} \end{bmatrix}^T \qquad \text{(B-2)}$$
$$y_i(t) = \beta \Delta f \quad \forall\ i = 1,2,\dots N$$

$$A = \begin{bmatrix} A_{11} & A_{12} & \cdots & A_{1N} \\ A_{21} & A_{22} & \cdots & A_{2N} \\ \vdots & \vdots & \ddots & \vdots \\ A_{N1} & A_{N2} & \cdots & A_{NN} \end{bmatrix}$$

$$A_{ij} = \begin{bmatrix} 0 & 0 & \dots & 0 \\ 0 & 0 & \dots & 0 \\ \vdots & \vdots & \ddots & \vdots \\ -2\pi T_{ij} & 0 & \dots & 0 \end{bmatrix} \qquad \text{(B-3)}$$

$$A_{ii} = \begin{bmatrix} \frac{-D_i}{M_i} & \frac{1}{M_i} & 0 & 0 & \frac{1}{M_i} & \frac{-1}{M_i} \\ 0 & \frac{-1}{T_{ci}} & \frac{1}{T_{ci}} & 0 & 0 & 0 \\ \frac{-F_{pi}}{R_i T_{gi}} & 0 & \frac{-1}{T_{ri}} & \frac{T_{gi} - F_{pi} T_{ri}}{T_{ri} T_{gi}} & 0 & 0 \\ \frac{-1}{R_i T_{gi}} & 0 & 0 & \frac{-1}{T_{gi}} & 0 & 0 \\ 0 & 0 & 0 & 0 & \frac{-1}{T_{evi}} & 0 \\ 2\pi \sum_{j=1, j \neq i}^{N} T_{ij} & 0 & 0 & 0 & 0 & 0 \end{bmatrix} \qquad \text{(B-4)}$$

$$B_0 = \begin{bmatrix} B_{011} & 0 & \dots & 0 \\ 0 & B_{022} & \dots & 0 \\ \vdots & \vdots & \ddots & \vdots \\ 0 & 0 & \cdots & B_{0NN} \end{bmatrix}$$

$$B_i = \begin{bmatrix} 0 & \dots & 0 & \dots & 0 \\ \vdots & \ddots & \vdots & \ddots & \vdots \\ 0 & \dots & B_k & \dots & 0 \\ \vdots & \ddots & \vdots & \ddots & \vdots \\ 0 & \dots & 0 & \dots & 0 \end{bmatrix} \qquad \text{(B-5)}$$

$$B_{0ii} = \begin{bmatrix} 0 & 0 & \frac{F_{pi}\alpha_{0i}}{T_{gi}} & \frac{\alpha_{0i}}{T_{gi}} & 0 & 0 \end{bmatrix}^T$$

$$B_k = \begin{bmatrix} 0 & 0 & 0 & 0 & \frac{K_{evi}\alpha_{1i}}{T_{evi}} & 0 \end{bmatrix}^T$$

$$C = diag\begin{bmatrix} C_1 & C_2 & \dots & C_N \end{bmatrix}$$
$$C_i = \begin{bmatrix} \beta_i & 0 & 0 & 0 & 0 & 0 \end{bmatrix}^T \qquad \text{(B-6)}$$

$$F = diag\begin{bmatrix} F_1 & F_2 & \dots & F_N \end{bmatrix}$$
$$F_i = \begin{bmatrix} \frac{-1}{M_i} & 0 & 0 & 0 & 0 & 0 \end{bmatrix}^T \qquad \text{(B-7)}$$

## REFERENCES

[1] L. Erickson, “Reducing greenhouse gas emissions and improving air quality: Two global challenges”, *Environ. Prog. Sustainable Energy*, vol. 36, pp. 982-988, 2017.

[2] F. Salah, J. Ilg, C. Flath, H. Basse and C. Dinther, “Impact of electric vehicles on distribution substations: A Swiss case study”, *Appl. Energy*, vol. 137, pp.88-96, 2015.

[3] H. Rashidizadeh, H. Najafi, A. Moghaddam and J. Guerrero, “Optimal decision making framework of an electric vehicle aggregator in future and pool markets”, *J. Oper. Autom. Power Eng.*, vol. 6, pp. 157-168, 2018.

[4] K. Hedegaard, H. Ravn, N. Juul and P. Meibom, “Effects of electric vehicles on power systems in Northern Europe”, *Energy*, vol. 48, pp.356-368, 2012.

[5] H. Lund and W. Kempton, “Integration of renewable energy into the transport and electricity sectors through V2G”, *Energy Policy*, vol. 36, pp. 3578-3587, 2008.

[6] K. Tan, V. Ramachandaramurthy and J. Yong, “Integration of electric vehicles in smart grid: A review on vehicle to grid technologies and optimization techniques”, *Renewable Sustainable Energy*, vol. 53, pp.720-732, 2016.

[7] M. Sarker, Y. Dvorkin and M. Vazquez, “Optimal participation of an electric vehicle aggregator in day-ahead energy and reserve markets”, *IEEE Trans. Power Syst*., vol. 31, pp. 3506-3515, 2016.

[8] A. Akbarimajd, M. Olyaee, H. Shayeghi and B. Sobhani, “Distributed multi-agent load frequency control for a large-scale power system optimized by grey wolf optimizer, *J. Oper. Autom. Power Eng.*, vol. 5, pp. 151-162, 2017.

[9] S. Saxena, “Load frequency control strategy via fractional-order controller and reduced-order modeling”, *Elect Power & Energy Syst*., vol. 104, pp. 603-614, 2019.

[10] H. Jia, X. Li, Y. Mu, C. Xu, Y. Jiang, X. Yu, J. Wu and C. Dong, “Coordinated control for EV aggregators and power plants in frequency regulation considering time-varying delays”, *Applied Energy*, vol. 210, pp. 1363-1376, 2018.

[11] T. Pham and H. Trinh, “Load frequency control of power systems with electric vehicles and diverse transmission links using distributed functional observers”, *IEEE Trans. Smart Grid*, vol. 7, pp. 238-252, 2016.

[12] H. Liu, Z. Hu, Y. Song, J. Wang and X. Xie, “Vehicle-to-grid control for supplementary frequency regulation considering charging demands”, *IEEE Trans. Power Syst*., vol. 30, pp. 3110-3119, 2015.

[13] T. Masuta and A. Yokoyama, “Supplementary load frequency control by use of a number of both electric vehicles and heat pump water heaters”, *IEEE Trans. Smart Grid*, vol. 3, pp. 1253-1262, 2013.

[14] M. Gheisarnejad and M. Khooban, “Secondary load frequency control for multi-microgrids: HiL real-time simulation”, *Soft Comput*., vol. 23, pp. 5785–5798, 2019.

[15] H. Ali, G. Magdy, B. Li, G. Shabib, A. Elbaset, D. Xu and Y. Mitani, “A new frequency control strategy in an islanded microgrid using virtual inertia control-based coefficient diagram method”, *IEEE Access.*, vol. 7, pp.16979- 16990, 2019.

[16] M. Khooban, T. Niknam, M. Shasadeghi, T. Dragicevic and F. Blaabjerg, “Load frequency control in microgrids based on a stochastic noninteger controller”, *IEEE Trans. Sustainable Energy*, vol. 9, pp. 853-861, 2018.

[17] A. Safari, F. Babaei and M. Farrokhifar, “A load frequency control using a PSO-based ANN for micro-grids in the presence of electric vehicles”, *Int. J. Ambient Energy*, pp.1-13, 2019.

[18] T. Pham, S. Nahavandi, H. Trinh and K. Wong, “Static output feedback frequency stabilization of time-delay power systems with coordinated electric vehicles state of charge control”, *IEEE Trans. Power Syst.*, vol. 32, pp. 3862-3874, 2017.

[19] S. Debbarma and A. Dutta, “Utilizing electric vehicles for LFC in restructured power systems using fractional order controller”, *IEEE Trans. Smart Grid*., vol. 8, pp. 2554-2564, 2017.

[20] H. Fan, L. Jiang, C. Zhang and C. Mao, “Frequency regulation of multi-area power systems with plug-in electric vehicles considering communication delays”, *IET Gener. Transm. Distrib.*, vol. 10, pp. 3481-3491, 2016.

[21] S. Debbarma and A. Dutta, “Utilizing electric vehicles for LFC in restructured power systems using fractional order controller”, *IEEE Trans. Smart Grid*, vol. 8, pp. 2554-2564, 2017.

[22] V. Çelik, M. Özdemir and G. Bayrak, “The effects on stability region of the fractional-order PI controller for one-area time-delayed load–frequency control systems”, *Trans. Inst. Meas. Control*, vol. 39, pp. 1509-1521, 2017.

[23] P. Ojaghi and M. Rahmani, “LMI-based robust predictive load frequency control for power systems with communication delays”, *IEEE Trans. Power Syst*., vol. 32, pp. 4091-4100, 2017.

[24] K. Ko and D. Sung, “The effect of EV aggregators with time-varying delays on the stability of a load frequency control system," *IEEE Trans. Power Syst*., vol. 33, pp. 669-680, 2018.

[25] S. Mirjalili, “SCA: a sine cosine algorithm for solving optimization problems”. *Knowl. Syst*., vol. 96, pp. 120-133, 2016.

[26] R. Khezri, A. Oshnoei, M. Tarafdar and S. Muyeen, “Coordination of heat pumps, electric vehicles and AGC for efficient LFC in a smart hybrid power system via SCA-based optimized FOPID controllers”, *Energies*, vol. 11, pp. 420-441, 2018.